# MAGNESIA POROUS PARTICLE SEPARATORS FOR LITHIUM–ALUMINUM/IRON SULFIDE BATTERIES

YASUTOSHI SHIMIZU, MASANAO TERASAKI and SHIN KASHIHARA

*Advanced Battery Laboratory, Corporate R & D Center, Japan Storage Battery Co., Ltd., 601, Kyoto (Japan)*

(Received February 16, 1984; accepted May 7, 1984)

## Summary

Magnesium oxide porous particles (~200 μm) made by sintering a fine powder of MgO with $Mg(NO_3)_2$ as the binder, have been evaluated as the separator of Li–Al/FeS cells. Physical properties, such as distribution of porosity and compressibility, were determined. In-cell tests with 25 A h cells and post-test examination of the separator indicated that the MgO porous particle separator possesses low ionic impedance as well as high compressive strength. This new material, being far less expensive than the commonly used boron nitride felt, has a fair possibility of replacing it for use in Li–Al/FeS systems.

## Introduction

High-temperature molten salt Li–Al/LiCl–KCl/$FeS_x$ cells, which are noted for their high energy density and superior safety [1, 2], are being developed for energy storage in electric utility systems by a number of institutions.

Identification of low cost separators is one of the key factors for the successful commercialization of these batteries. Boron nitride (BN) felt separators have been demonstrated in engineering tests [3, 4] to be adequate for this application. This separator has high porosity (~90%) and, hence, low ionic impedance, in addition to excellent compatibility with other cell materials at the operating temperature of 470 °C. However, it is too costly [5], and insufficiently strong mechanically to prevent electrode shape change during cell operation [6].

The search for less expensive separators has led to the development of MgO, $Y_2O_3$ and AlN powder separators [7 - 9]. Cell assembly with such powder separators is simple and amenable to mass production. Although powder separators were shown to maintain their integrity and conform to small dimensional changes of electrodes [7], their porosity (~50%) is considerably lower than that of BN felt and this drawback would probably limit

0378-7753/84/$3.00 

their application to stationary load-levelling systems operating only at low current densities [7].

This report describes a new type of separator. The MgO porous particle separator, which possesses both the high porosity of BN felt and the high mechanical resistance of powder separators, and is a promising candidate for the separator of Li–Al/FeS cells.

## Experimental

*Fabrication of MgO porous particles*

Fine MgO powder with an average particle size of 0.3 $\mu$m was used as the starting material.

A mixture of 100 g of MgO powder and 160 ml of 0.3M aqueous solution of $Mg(NO_3)_2$ was dried and the residue crushed and granulated into particles 200 $\mu$m in diameter. The granules, containing $Mg(NO_3)_2$ at 2 mol%, were first calcined at 600 °C. In this process, $Mg(NO_3)_2$ was decomposed and the resulting active MgO served as the binder. The granules were then fired at 1000 °C and, after cooling, sieved to a screen size range of 100 - 200 mesh.

Cumulative pore-volume distribution of the particles was measured with a mercury porosimeter. The particles were subjected to scanning electron microscopy to confirm the particle size and to visually inspect the shape and the microstructure of the particles.

Compressibility was measured by pressing the particles in a 28.5 mm dia. die.

For comparison, parallel measurements were made for BN felt and MgO powder separators. The latter was made from fused MgO sieved to 100 - 200 mesh.

*In-cell test of separators*

An exploded view of the bi-cells used for separator testing is shown in Fig. 1. The outer dimensions were 72 × 32 × 90 mm. The capacity of the cell, limited by the positive electrode, was 25 A h. The positive electrode measured 57 × 57 mm and was 7 mm in thickness. The opposing negative electrodes had the same dimensions, except for the thickness (6 mm). A mixture of LiCl and KCl (54 wt.% LiCl) was used as the electrolyte. The active materials of each of the electrodes, in the charged state, were mixed with the electrolyte and cold-pressed into honeycomb-shaped current collectors. The electrode plaques thus formed were then placed in electrode frames with welded, stainless-steel screens on each side.

Magnesium oxide porous particle separators or MgO powder separators were made by simply pouring the material into the gap formed by the electrodes and spacers, which were inserted in the cell case in advance. The spacers were made from BN plates, which are far less expensive than BN felt. When using BN felt separators, approximately 10 mg/cm$^2$ of MgO was deposited by decomposition of $Mg(NO_3)_2$ at 600 °C to improve the wettability of the felt by the molten electrolyte.

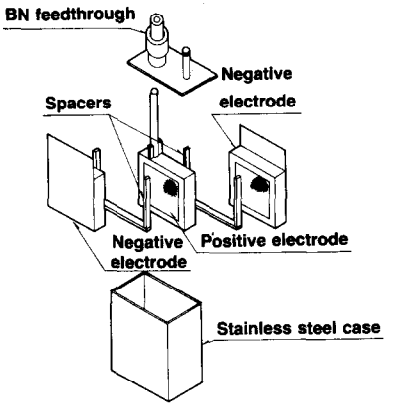


Fig. 1. Cell assembly.

After filling the cell with additional molten electrolyte, the cell case was welded at the upper edges and the positive electrode was sealed with a conventional BN feedthrough.

The cells were placed in inert gas atmosphere furnaces and cycled continuously at 470 °C between the cut-off potentials of 1.0 and 1.55 V. The charge current was held constant at 2.5 A (37 mA/cm$^2$) while the discharge current was varied from 2.5 A to 10 A (154 mA/cm$^2$).

After 200 cycles of charge and discharge, the cells were dismantled and subjected to optical microscopy, scanning electron microscopy and X-ray microanalysis to identify any morphological change in the separators.

## Results and discussion

### *Physical characteristics*

The physical characteristics of various separators are compared in Table 1. Boron nitride felt separators are featured with high porosity and

TABLE 1

Physical characteristics of various separators

| Type | Porosity (%) | Av. pore diameter ($\mu$m) | Loading density (g/cm$^3$) | Compressibility (% decline/kg cm$^{-2}$) |
|---|---|---|---|---|
| BN felt* | 89 | 24 | 0.27 | 3.2 |
| MgO porous particle** | 84 | 22 (0.10) | 0.58 | 1.1 |
| MgO powder*** | 53 | 28 | 1.72 | 1.5 |

*Treated with $Mg(NO_3)_2$ at 600 °C to promote wettability.
**100 - 200 mesh.
***Fused MgO, 100 - 200 mesh.

low loading density. In other words, batteries with BN felt separators are expected to exhibit better high rate performance and higher energy density. However, as shown in Fig. 2, about 70% of the pores of BN felt separators were found to be larger than 20 $\mu$m, which is the upper limit of the pore size required to prevent inadvertent migration of the particulate active materials through the separators [10].

Electrodes of Li–Al/FeS cells are known to swell with cycle operations. The compressibility test results shown in Fig. 3 indicate that the porosity of BN felt is easily reduced by the enlargement of the electrodes or BN felt has a lesser capability in deterring electrode swelling.

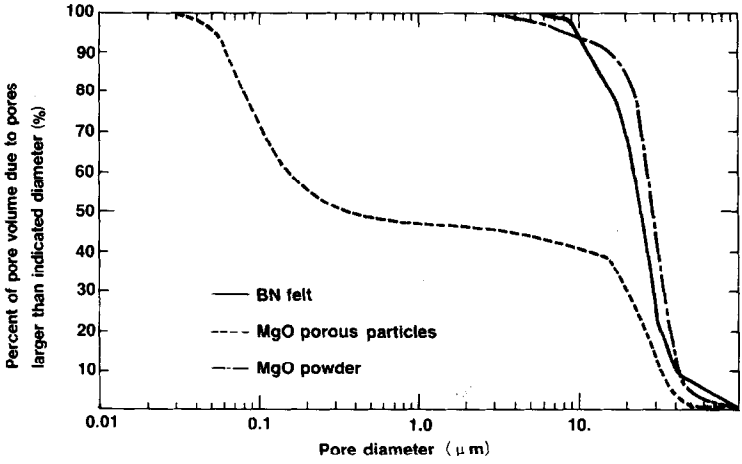


Fig. 2. Pore size distribution.

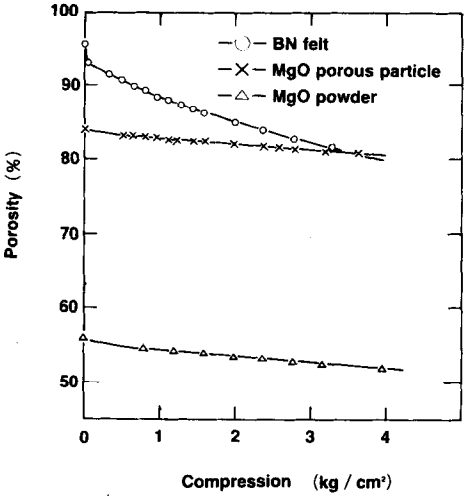


Fig. 3. Change in separator porosity with compression.

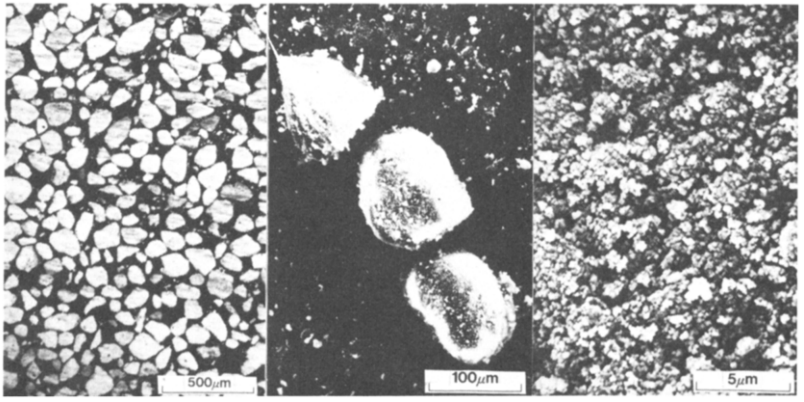


Fig. 4. Scanning electron micrograph of MgO porous particles.

Magnesium oxide powder separators maintain dimensional integrity under compression (Fig. 3), but they are far denser and less porous (Table 1).

Magnesium oxide porous particle separators have high porosity, comparable with BN felt separators. Pore volume distribution, shown in Fig. 2, indicates clearly that there are two kinds of pores; larger pores (~20 μm) attributable to the void space formed by adjacent particles, and smaller pores (~0.1 μm) corresponding to the dimension of the starting powders. The existence of the latter pores within each particle explains the large difference in porosity between MgO porous particle separators and MgO powder separators (Table 1). The fraction of pores larger than the aforementioned threshold value (20 μm) is less than one half of that found with BN felt separators, and so the new separators are supposedly more effective in providing active material particle retention. Examination by SEM corroborates the above arguments about pore size (Fig. 4).

Magnesium oxide porous particles can maintain dimensional integrity under compression: the compression curve for these particles remained linear up to 30 kg/cm$^2$ of compression. This means that the microstructure of the particles was intact up to that yielding pressure, which far exceeds the swelling pressure (2.3 kg/cm$^2$) generated under ordinary cell operational conditions [11].

*Cell performance*

The cell performance parameters measured were average discharge voltage, coulombic efficiency, and utilization of active materials. The latter is defined as the fraction of the theoretical capacity that could actually be discharged. Table 2 lists the specifications of the test cells.

Figure 5 illustrates the relationship between average discharge voltage and current density. The cells with BN felt separators exhibited characteristics almost identical with those using MgO porous particle separators, but the cell with MgO powder separators showed definitely inferior characteristics,

TABLE 2

Description of cells* with various separators

| Cell no. | Separator | | | Theoretical capacity (A h) | Electrode loading density | | Cell weight (g) |
|---|---|---|---|---|---|---|---|
| | Type | Thickness (mm) | Porosity (%) | | Positive (A h/cm$^3$) | Negative (A h/cm$^3$) | |
| P-25-4 | BN felt** | 2.0 | 89 | 24.5 | 1.10 | 0.76 | 564 |
| P-25-5 | BN felt** | 2.0 | 89 | 24.2 | 1.10 | 0.76 | 570 |
| P-25-6 | MgO porous particle*** | 2.0 | 84 | 24.7 | 1.10 | 0.76 | 580 |
| P-25-8 | MgO powder† | 2.0 | 53 | 24.2 | 1.10 | 0.76 | 622 |
| P-25-13 | MgO porous particle*** | 2.0 | 84 | 24.1 | 1.10 | 0.76 | 585 |

*Cell size: 72 x 32 x 90 mm.
**2 ply, with MgO (10 mg/cm$^2$).
***100 - 200 mesh.
†Fused MgO, 100 - 200 mesh.

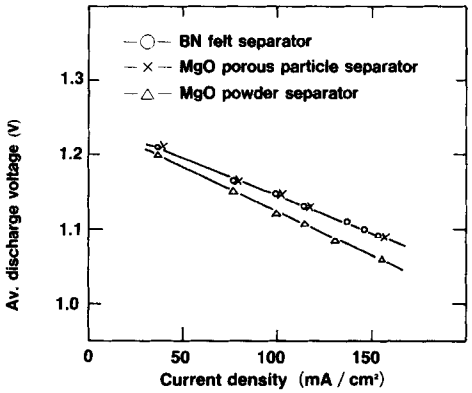


Fig. 5. Average discharge voltage *vs.* current density for 25 A h cells.

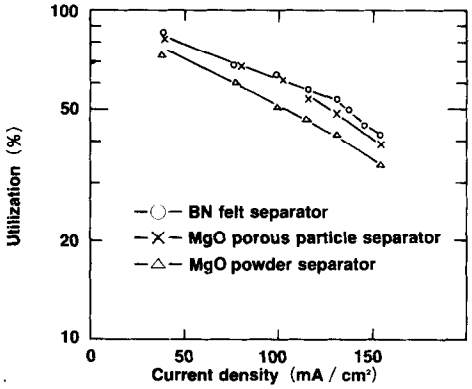


Fig. 6. Utilization *vs.* current density for 25 A h cells.

especially at higher current densities. Based on the facts that the porosities of the former two separators were nearly equal, while the particle sizes of the latter two separators were nearly equal, it is safe to assume that the inner voids of the MgO porous particles were effectively acting as ionic conduction paths.

As shown in Fig. 6, utilization of the positive active material was again strongly dependent on the porosity. The performance of MgO porous particle separators compared well with that of BN felt separators up to about 100 mA/cm$^2$ (3 h rate).

Durability test results of a cell with MgO porous particle separators are shown in Figs. 7 and 8. Satisfactory coulombic efficiency (>98%) was

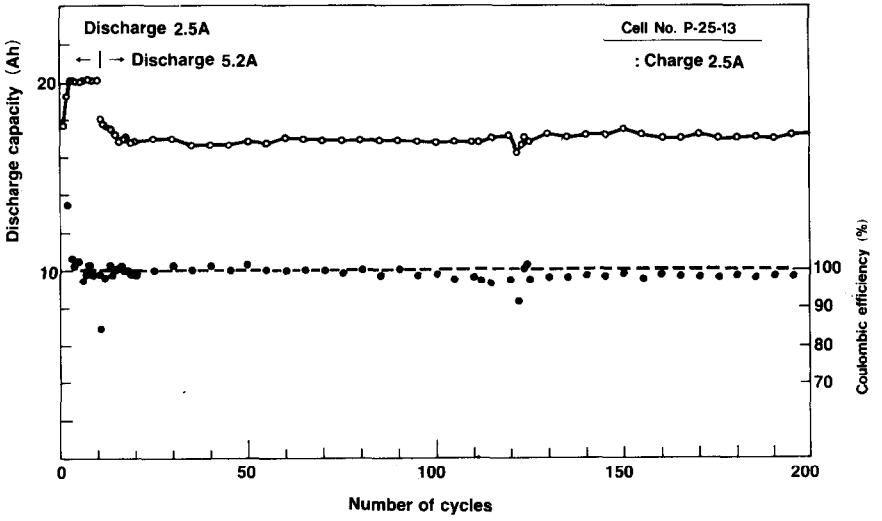


Fig. 7. Cycle life performance of 25 A h cell with MgO porous particle separators.

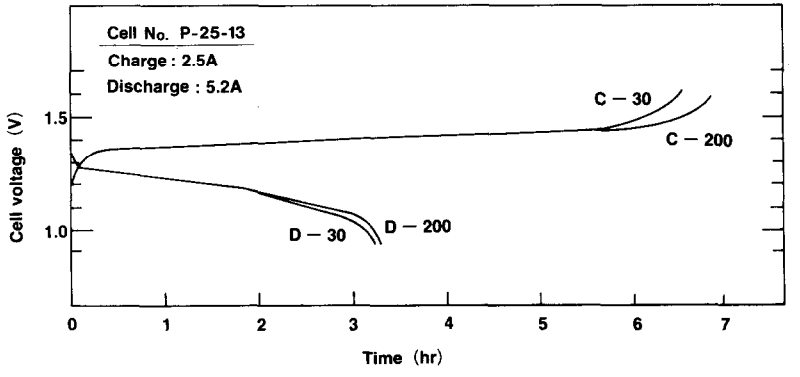


Fig. 8. Charge–discharge curves of 25 A h cell with MgO porous particle separators at the 30th and 200th cycle.

maintained throughout the operating life, and no capacity reduction trend was observed.

It may be noted that the cells were not designed to optimize energy density. Since the size of the cells was small, the cell case and the feed-through accounted for about 40% of the cell weight.

*Post-test examination*

Durability tests of all the cells were terminated after 200 charge and discharge cycles and the cells were dismantled for post-test examinations, the results of which are summarized in Table 3.

A cross-section of a cell with BN felt separators, shown in Fig. 9, reveals extensive deformation of both electrodes. The central part of the negative electrode had expanded approximately 20% more than the peripheral parts,

TABLE 3

Results of post-test examination of cells after 200 cycles

| Separator type | Chemical stability | Compressibility | Particle retention |
|---|---|---|---|
| BN felt | No chemical reaction | ~60% compression | Negative active material and iron particles were dispersed into 80% of separators |
| MgO porous particle | No chemical reaction | No dimensional or microstructural change | A small amount of iron particles were dispersed into 15% of separators |
| MgO powder | No chemical reaction | No dimensional or microstructural change | A small amount of iron particles were dispersed into 15% of separators |

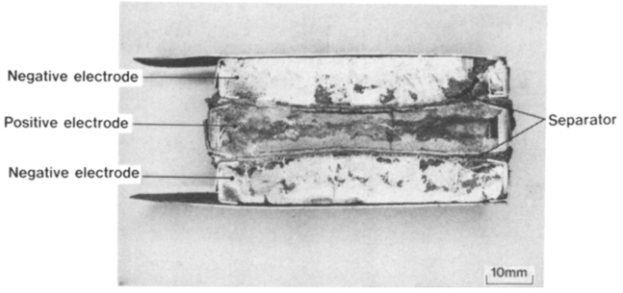


Fig. 9. Cross section of cell P-25-4 with BN felt separators.

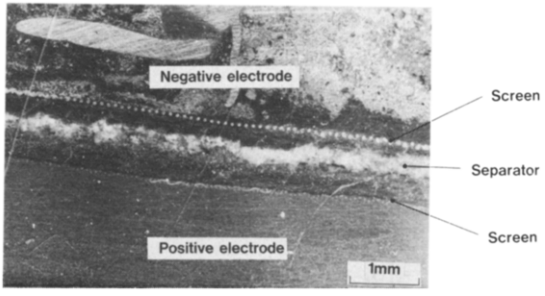


Fig. 10. Typical section of BN felt separator from cell No. P-25-4.

while swelling of the positive electrode ranged from nil near the center to 40% at the edges. The separators were compressed to 60% of the original thickness. Figure 10 shows a photomicrograph of a section of the BN felt separator. The negative active material and iron particles, a discharge product of the positive electrode, are seen to have infiltrated well into the separator, traversing the stainless-steel screens. The chemical species of the penetrant were identified by X-ray microanalysis and X-ray diffraction. Only 20% of

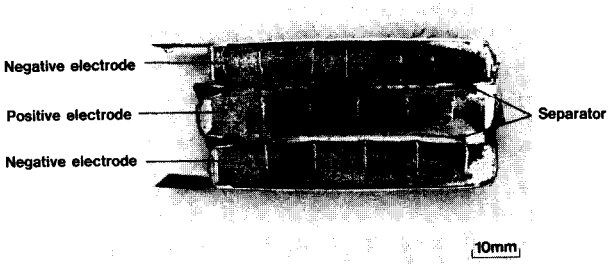


Fig. 11. Cross section of cell P-25-13 with MgO porous particle separators.

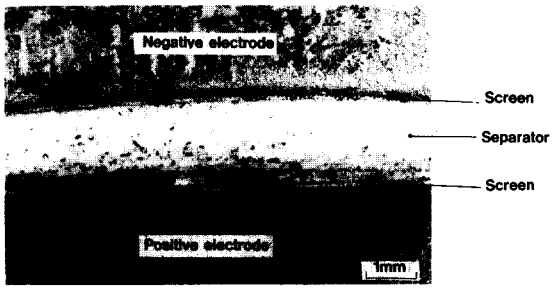


Fig. 12. Typical section of MgO porous particle separator from cell No. P-25-13.

the thickness of the separator was found to be free of penetration materials — a situation conducive to short circuiting.

Figure 11 shows a section of a cell with MgO porous particle separators after 200 cycles. Distortion of the electrodes and reduction of the separator thickness are not observed. This indicates a sufficiently high compressive strength of this separator material. No evidence of particle rearrangement was seen from metallographic inspection of the separator (Fig. 12) and no removal of the particles from the separator region into the upper open space of the cell was detected. The contributing factors for the low particle mobility could be the irregular edge shape of the particles and the absence of excessive electrolyte within the separator.

Intrusion of the negative active material was prevented at the boundary, while iron particles were seen to have penetrated into the separator. However, the penetration was limited to the zone immediately adjacent to the positive electrode, and about 85% of the separator was immune to the penetrant.

Magnesium oxide porous particles were chemically compatible with other materials in the environment of the operating cells.

## Conclusion

Magnesium oxide porous particles were prepared by loosely sintering fine MgO powder with $Mg(NO_3)_2$ as the binder. The particles thus formed

showed excellent performance as the separators of Li–Al/FeS cells. The preparation of the particles and fabrication of the separators are very simple processes. This, together with the low costs of the starting materials, offers a path to cost-effective production of Li–Al/FeS batteries.

## Acknowledgement

The authors are grateful to Dr H. Shimotake of Argonne National Laboratory for his advice and encouragement.

## References

1 D. L. Barney, R. K. Steunenberg, A. A. Chilenskas, E. C. Gay, J. E. Battles, W. E. Miller, D. R. Vissers, H. Shimotake, R. Hudson, B. A. Askew, S. Sudar, F. C. Tompkins and J. S. Dunning, *Argonne Nat. Lab. Prog. Rep. ANL-80-128*, 1980.
2 R. Knödler, *Proc. 17th IECEC, Los Angeles, CA, Aug. 18 - 22, 1982*, IEEE, pp. 552 - 556.
3 F. J. Martino, E. C. Gay and W. E. Moore, *J. Electrochem. Soc., 129* (1982) 2701.
4 F. J. Martino, E. C. Gay and H. Shimotake, *Proc. 15th IECEC, Seattle, WA, Aug. 18 - 22, 1980*, Am. Inst. Aero. and Astro., pp. 205 - 210.
5 A. A. Chilenskas, J. C. Shaefer, W. L. Towle and D. L. Barney, *Argonne Nat. Lab. Prog. Rep. ANL-79-59*, 1979.
6 R. B. Swaroop and J. E. Battles, *J. Electrochem. Soc., 128* (1981) 1873.
7 J. P. Mathers, C. W. Boquist and T. W. Olszanski, *J. Electrochem. Soc., 125* (1978) 1913.
8 G. Bandyopadhyay, R. B. Swaroop and J. E. Battles, *J. Electrochem. Soc., 129* (1982) 2187.
9 L. R. McCoy, R. S. Saunders, L. A. Heredy and S. Sudar, *Proc. 16th IECEC, Atlanta, GA, Aug. 9 - 14, 1981*, Am. Soc. Mech. Eng., pp. 747 - 751.
10 J. E. Battles, F. C. Mrazek and N. C. Otto, *Argonne Nat. Lab. Rep. ANL-80-130*, 1980.
11 D. L. Barney, R. K. Steunenberg, A. A. Chilenskas, E. C. Gay, J. E. Battles, R. Hudson, B. A. Askew and F. C. Tompkins, *Argonne Nat. Lab. Prog. Rep. ANL-81-65*, 1981.